Medical Engineering and Physics 64 (2019) 15–22

Contents lists available at ScienceDirect

Medical Engineering and Physics

journal homepage: www.elsevier.com/locate/medengphy

Towards viscoelastic characterisation of the human ulnar nerve: An early assessment using embalmed cadavers

Carla G Barberio[a], Tahseen Chaudhry[b], Dominic M Power[b], Simon Tan[b], Bernard M Lawless[c], Daniel M Espino[c,*], Joanne C Wilton[a]

[a] Department of Anatomy, College of Medical and Dental Sciences, University of Birmingham, United Kingdom
[b] Hand and Peripheral Nerve Research Network Birmingham, Queen Elizabeth Hospital, University Hospitals Birmingham, United Kingdom
[c] Department of Mechanical Engineering, University of Birmingham, Birmingham B15 2TT, United Kingdom

ARTICLE INFO

Article history:
Received 2 May 2018
Revised 22 November 2018
Accepted 4 December 2018

Keywords:
Dynamic mechanical analysis
Frequency
Human
Ulnar nerve
Viscoelasticity

ABSTRACT

Cubital tunnel syndrome is the most prevalent neuropathy of the ulnar nerve and its aetiology is controversial. Potential replacement materials should display similar viscoelastic properties. The purpose of this study was to assess the feasibility and merit of quantifying the frequency-dependent viscoelastic properties of proximal and distal sections of the human ulnar nerve. Four ulnar nerves ($n = 4$) were dissected from the elbows of human cadavers and sectioned at the level of the cubital tunnel into proximal and distal sections. These eight sections of the ulnar nerve were sinusoidally loaded to induce stresses between 0.05 and 0.27 MPa and the viscoelastic properties were measured between 0.5 and 24 Hz using dynamic mechanical analysis. The nerves were found to exhibit frequency-dependent viscoelastic behaviour throughout this frequency range. The median storage moduli of the proximal nerves ranged between 7.03 and 8.18 MPa, and 8.85–10.19 MPa for distal nerves, over the frequency-sweep tested. The median loss moduli of the proximal nerves ranged between 0.46 and 0.81 MPa and between 0.51 and 0.80 MPa for distal nerves. Ulnar nerves display frequency dependency viscoelasticity. Such characterisation is feasible with potential applications to suitable nerve grafts.

1. Introduction

The ulnar nerve travels through the upper limb and cubital tunnel transmitting sensation from the skin overlying the hypothenar eminence, the corresponding area of skin posteriorly, the little finger and half of the ring finger as well as supplying motor function to numerous muscles of the forearm and hand [1]. Cubital tunnel syndrome is the most prevalent neuropathy of the ulnar nerve and the second commonest neuropathy of the upper limb [2]. Its aetiology is controversial. Originally, it was thought to be due to a compressive or entrapment neuropathy [3–5]. However, more recently, it has been thought to be due to nerve strain [2,6–9].

Studies have found that at certain levels of strain (6–16%), blood flow to the nerve and conduction of impulses by the nerve were reduced or even arrested [10–13]. In terms of nerve conduction, it has been shown that a 6% increased nerve strain for longer than an hour led to 70% decreased conduction velocity while a 12% increase in strain led to completely arrested nerve conduction in a study on rabbit nerves [13]. The nerve conduction returned once the above strains were removed [13]. In terms of blood flow, a 50% reduction was induced by 8% strain in a rat's sciatic nerve while an 80% reduction in blood flow was caused by 15% nerve strain [12]. Blood flow was completely blocked by 16% strain in a rabbit sciatic nerve [11]. Therefore, for adequate nerve function, nerve strain must be minimised. It has previously been shown that during normal motion of the elbow and shoulder joints, strain is applied dynamically to the ulnar nerve to levels that could result in both impaired conduction and perfusion [8,14,15].

Human peripheral nerves are known to exhibit viscoelastic properties [16] and this has been demonstrated for the human ulnar nerve by performing *in vitro* stress relaxation tests [17]. Unlike creep and stress relaxation, Dynamic Mechanical Analysis (DMA) is a dynamic testing method used to determine the viscoelastic properties of a material or multi-component structure [18]. DMA involves the application of an oscillating force to a specimen and measuring the out-of-phase displacement [19]. This gives time-dependent strain, $\varepsilon(t)$ (Eq. (1)), developed in response to the induced time-dependent stress, $\sigma(t)$, and the complex (dynamic)

* Corresponding author.
E-mail addresses: CGB358@student.bham.ac.uk (C.G. Barberio), tahseen.chaudhry@uhb.nhs.uk (T. Chaudhry), dominic.power@uhb.nhs.uk (D.M. Power), Simon.Tan@uhb.nhs.uk (S. Tan), B.M.Lawless@bham.ac.uk (B.M. Lawless), d.m.espino@bham.ac.uk (D.M. Espino), J.C.Wilton@bham.ac.uk (J.C. Wilton).

https://doi.org/10.1016/j.medengphy.2018.12.009
1350-4533/

Table 1
Ulnar nerve specimens.

Cadaver ID	Donor Age	Gender	Side
Cadaver 1	90	Male	Right
Cadaver 1	90	Male	Left
Cadaver 2	89	Male	Left
Cadaver 3	75	Female	Left

modulus, $E^*(\omega)$ [20]:

$$\varepsilon(t) = \frac{\sigma(t)}{E^*(\omega)} \tag{1}$$

The viscoelasticity of a material can be characterised in terms of storage and loss moduli [20–22]. The storage modulus (E') characterises the ability of the material to store energy that is then available for elastic recoil; while, the loss modulus (E'') characterises the material's ability to dissipate energy. The storage and loss moduli are related to E^* and the phase angle (δ) by Eq. (2) and (3), respectively [20,22,23]:

$$|E^*| = \sqrt{E'^2 + E''^2} \tag{2}$$

$$\delta = \tan^{-1}\left(\frac{E''}{E'}\right) \tag{3}$$

To the authors' knowledge, the understanding of frequency-dependent viscoelastic properties of human ulnar nerve is currently absent. As the ulnar nerve is viscoelastic, and exposed to dynamic loading, its frequency-dependency requires characterisation. Furthermore, any potential replacement materials (allograft, synthetic grafts, etc.) should display similar viscoelastic properties. Moreover, frequency-dependent viscoelastic properties are important because if these measurements are used to infer the *in vivo* strain, then the strain itself would be highly sensitive to the rate of loading: of importance given the dynamic loading to which the ulnar nerve is exposed *in vivo*. Additionally, mechanical behaviour of viscoelastic biomaterials may differ considerably between physiological and sub-physiological loading rates [24].

The aim of this study was to assess the feasibility and merit of quantifying the frequency-dependent viscoelastic properties of proximal and distal sections of the human ulnar nerve. Furthermore, this study subsequently compared the ulnar nerve frequency-dependency viscoelastic properties of storage and loss moduli proximally and distally to the cubital tunnel. Given the limited availability of fresh human ulnar nerves for mechanical testing, embalmed human nerves have been used.

2. Materials and methods

2.1. Cadaver information and ulnar nerve specimen preparation

Four ulnar nerves were dissected and surgically removed from four elbows of three whole, intact embalmed cadavers (Table 1). Ethical approval was obtained from the Human Tissue Authority according to the Human Tissue Act (2004) under the University of Birmingham license (number 12236) with the donors consenting to the use of their cadavers for education and research. All tissues were obtained following the Declaration of Helsinki ethical principles.

The elbows were first marked and incised to expose the nerves. Sutures were then placed at approximately 20 mm or 30 mm (due to anatomical positioning). Biomechanical tests consisting of flexion and extension of the elbow at varying degrees of shoulder abduction were performed as part of a separate study [15]. The nerves were removed from the cadaver then wrapped and soaked in a damping down solution containing H_2O, Poly(ethylene glycol) 8000, biocleanse (Fisher Scientific, Loughborough, UK) and Industrial Methylated Spirits (IMS) (VWR International Ltd, Leighton Buzzard, UK). Next, the nerves were double bagged as whole nerves. Each nerve was approximately 20–30 cm in length. The nerves were then sectioned (Fig. 1), at the level of the cubital tunnel into proximal and distal sections. Three nerves were divided into 40 mm sections, (approximately 20 mm of a gauge and two 10 mm shoulder sections used to grip the nerve for mechanical testing) and one nerve was divided into 50 mm sections, (approximately 30 mm of a gauge and two 10 mm shoulder sections). The difference in length was to maintain consistent suture positioning from a previous study [15]. Specimens were hydrated with the aforementioned damping down solution. Branches were removed with the nerves. The nerves were then mechanically tested the following day at room temperature.

2.2. Preliminary tests

BOSE Electroforce DMA Grips (Bose Corporation, ElectroForce Systems Group, Minnesota, USA), were used to grip 10 mm on either side of the nerve. Preliminary ramp tests were conducted on two specimens from one cadaver (taken 10 cm proximal to and 10 cm distal to the cubital tunnel) of approximately 20 mm of a gauge of proximal and distal sections of all nerves. These samples were extended at a linear translational rate of 0.05 mm/s in accordance with a previous study [17] to characterise the quasi-static stress-strain curves of the human nerves (ulnar proximal and distal). Tensile tests were performed at an initial ramp up strain of 10% [17]. A Vernier calliper was used to measure height and diameter of each nerve specimen. As the nerves were approximately elliptical in cross-sectional area, three sagittal (a) and three coronal (b) radii were measured and averaged, respectively, to calculate the elliptical cross-sectional area (A_e) using Eq. (4) [17].

$$A_e = \pi ab \tag{4}$$

Force versus displacement of proximal and distal nerves showed differences in stiffness (gradient of the line in N/mm) between the two nerve specimens (see Fig. 2). When comparing a linear region (often termed post-transitional), but avoiding any potential end-stage plastic deformation, the proximal human nerve was stiffer than the distal nerve (see Fig. 2). Calculating the stiffness of each nerve (as the force/extension within this linear range) led to values of 15.00 N/mm for the proximal human nerve and 8.07 N/mm for the distal nerve. Therefore, the DMA protocol devised included comparison of proximal and distal samples (Section 2.3).

Fig. 3a and b show stress versus strain of the proximal and distal human nerves. For the proximal nerve, 2% (0.02) strain was equivalent to 0.04 MPa stress while 6% (0.06) strain was equivalent to 0.15 MPa of stress (see Fig. 3a). However, 2% (0.02) strain, of the distal nerve, was equivalent to 0.05 MPa while 6% (0.06) strain was equivalent to 0.27 MPa of stress (see Fig. 3b).

At approximately 7–8% strain, the distal nerve began to demonstrate signs of damage, as evidenced by a plateau of the induced stress (see Fig. 3b), and may be associated with plastic deformation of the nerve and/or rupture. This plateau could mean that the microstructure of the nerve is rupturing. Therefore, the distal nerve's values of stress and strain were chosen to guide the DMA testing to avoid rupture in the actual experiment.

2.3. Dynamic mechanical analysis (DMA)

The viscoelastic properties of the nerve sections were characterised using a Bose ElectroForce 3200 testing machine running Bose WinTest 4.1 DMA software (Bose Corporation, ElectroForce

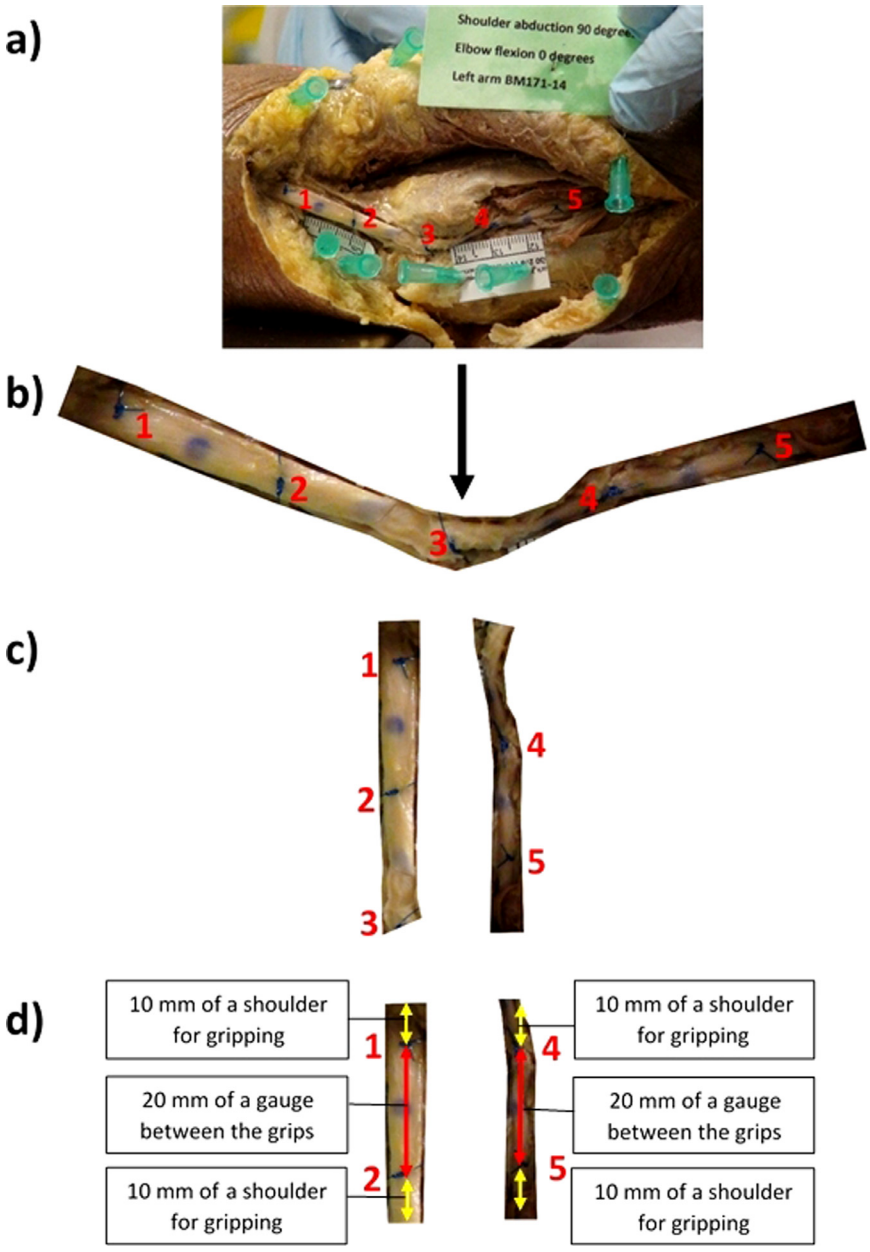

Fig. 1. BM 171-14 left ulnar nerve with (a) Five sutures marked in red numbers. (b) Left ulnar nerve with black arrow marking where it was sectioned at the cubital tunnel. (c) Left ulnar nerve proximal (left) and distal (right) sections. One section had 30 mm of a gauge with 10 mm for gripping at either end. (d) Final nerve sections for testing (lengths are approximate). (For interpretation of the references to colour in this figure legend, the reader is referred to the web version of this article.)

Systems Group, Minnesota, USA). DMA has previously been used to quantify the storage and loss properties of a variety of biological tissues [22,25–28] and orthopaedic implants [18,29].

For DMA, each nerve was sinusoidally loaded to induce stresses between 0.05 MPa (equivalent to 2% strain of the distal nerve stress-strain curve; Fig. 3) and 0.27 MPa. 2% strain was chosen as the lower strain boundary to mimic the nerve *in vivo* conditions [30–32]. As the elliptical area of the nerve varied, the applied force was calculated for each individual nerve specimen and the individual force ranges were applied to the individual specimens. Thus, the induced sinusoidal stress was consistent for all samples, varying from a trough of 0.05 MPa to a peak of 0.27 MPa. Preliminary data (Section 2.2), of the distal nerve (Fig. 3), demonstrated that 6% strain was equivalent to 0.27 MPa of stress (see Eq. (5) where σ is stress, F is the applied force and A_e is the area of an ellipse).

$$F = \sigma A_e \tag{5}$$

A preload condition, at 1 Hz for 28 cycles, was applied before the frequency sweep to ensure no stress relaxation affected the frequency sweep. Next, the storage (E') and loss (E'') moduli were evaluated for 9 frequencies (0.5, 1, 1.5, 2, 5, 10, 15, 20 and 24 Hz). E' and E'' were calculated using the WinTest DMA software. Following the application of the oscillating force, the out-of-phase displacement response is measured [19]. By performing a Fast Fourier Transform (FFT) of the sinusoidal load (F) and displacement (d) for each frequency, the magnitudes of the force (F^*), magnitude of the displacement (d^*), the phase lag (δ) and frequency (f) were quantified [18]. F^* and d^* were used to calculate the dynamic stiffness (k^*) using Eq. (6).

$$k^* = \frac{F^*}{d^*} \tag{6}$$

As the nerves were elliptical, a shape factor, S_c (Eq. (7)), was used to calculate E' and E'' of the nerves using Eqs. (8) and (9),

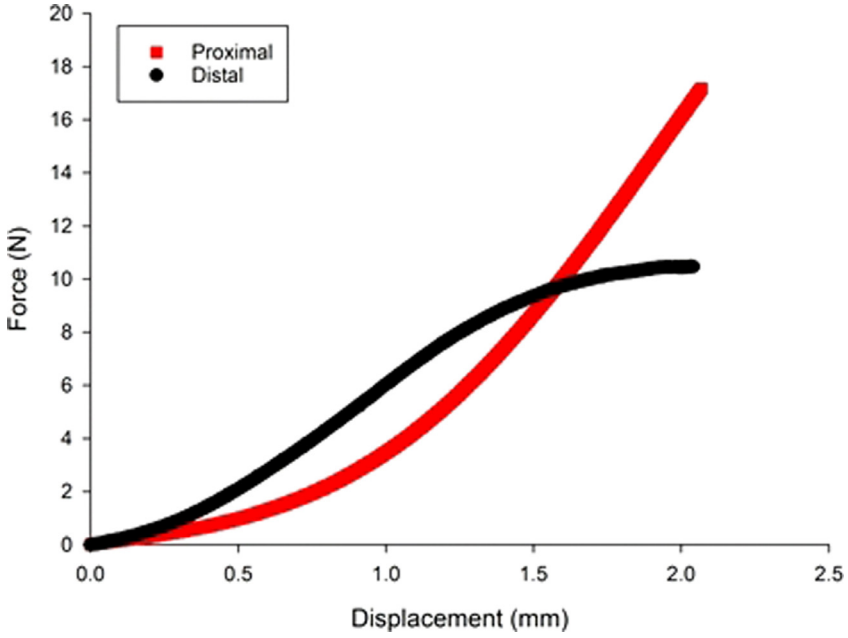

Fig. 2. Force (N) versus displacement (mm) of proximal and distal human nerves.

respectively. Eq. (7) uses a standard shape for a cylindrical sample [22,23], modified from a circular to an elliptical cross-section (see Eq. (4)); h refers to the gauge length ('height') of the specimen. The procedure used for measuring the preliminary specimens, which is described above (Section 2.2), was used to measure the specimens tested with DMA. The test gauge length of the specimens was 19.71 ± 1.26 mm with the exception of BM 172-14 in which a gauge length of 27.83 ± 2.61 mm was used as sutures were placed differently due to anatomical positioning.

$$S_c = \frac{\pi}{h}(ab) \tag{7}$$

$$E' = \frac{k^* \cos \delta}{S_c} \tag{8}$$

$$E'' = \frac{k^* \sin \delta}{S_c} \tag{9}$$

2.4. Data analysis

All statistical analyses were performed using SigmaPlot 13.0 (SYSTAT, San Jose, CA, USA). To evaluate the frequency-dependent viscoelastic behaviour of the nerves, regression analysis, was performed for E' and E''. A logarithmic fit (Eqs. (10) and (11)) was found to best fit the data, and was evaluated in terms of the significance of the curve fit ($p < 0.05$) and goodness of fit (R^2).

$$E' = A \ln(f) + B \tag{10}$$

$$E'' = C \ln(f) + D \tag{11}$$

The 95% confidence intervals were calculated for proximal sections ($n = 4$) and distal sections ($n = 4$). For comparisons of all nerves, confidence intervals error bars were calculated with a sample size of 8 ($n = 8$). A Wilcoxon ranked sum test was performed to evaluate the significant difference of the E', of the proximal and distal nerves for each frequency tested. This test was also performed to compare E'' of the proximal and distal nerves at each frequency tested. All statistical results with $p < 0.05$ were considered significant.

3. Results

The nerves displayed viscoelastic behaviour throughout the tested frequency range. Fig. 4 shows the frequency dependent trend of the E' of the proximal and distal sections of ulnar nerves. The median E' of the proximal nerves ranged between 7.03 and 8.18 MPa for the different frequencies tested. This compared to the range of the distal nerves' median E' which was between 8.85 and 10.19 MPa for the same frequency range. The frequency-dependency of the E' (Eq. (10)) was determined empirical to follow a logarithmic fit ($p < 0.05$). No significant difference was observed for E' between the proximal and distal sections across all frequencies tested ($p > 0.05$).

Fig. 4b shows the frequency dependent trend of the E'' of the proximal and distal sections of ulnar nerves. The E'' was lower than the E' for both proximal and distal sections of nerves at all tested frequencies. Over the same frequency range tested, the median value for E'' of the proximal nerve specimens ranged between 0.46 and 0.81 MPa while the range of median for the distal nerves was 0.51 and 0.80 MPa. No significant difference was observed between proximal and distal sections for E'' ($p > 0.05$). With the exception of the E'' for proximal BM 172-14, the frequency-dependency of the E'' (Eq. (11)) was empirically described by a logarithmic fit (Table 2). Individual fits for E' and E'' have been provided as supplementary data.

Fig. 5 shows the frequency dependent trend of the E' of all proximal and distal sections of the ulnar nerves combined. The confidence interval error bars approximately halve between E' and E'' of proximal and distal nerves and E' and E'' of all nerves due to doubling of the sample size. Fig. 5b shows the frequency dependent trend of the E'' of all proximal and distal sections of the ulnar nerves combined. The E'' was less than the E' for all sections of the nerves combined at all tested frequencies.

4. Discussion

This study has, for the first-time, demonstrated that human ulnar nerves display frequency-dependent viscoelastic properties. Embalmed nerves have been used to demonstrate the feasibility of characterising their viscoelastic properties throughout a

Table 2
Logarithmic regression of storage modulus (E′) and loss modulus (E″) for proximal and distal sections of nerves. The units of coefficients (A and C) and constants (B and D) are N/mm^2. Regression with a $p < 0.05$ were deemed significant.

Specimen ID	A	B	R^2	p value	C	D	R^2	p value
Proximal BM 176-14	0.32	7.80	0.98	<0.001	0.03	0.59	0.69	0.006
Proximal BM 172-14	0.25	6.07	0.65	0.009	0.09	0.42	0.41	0.063
Proximal BM 171-14 Left	0.33	9.99	0.98	<0.001	0.05	0.63	0.60	0.014
Proximal BM 171-14 Right	0.26	6.54	0.96	<0.001	0.03	0.41	0.72	0.004
Median of all proximal	**0.29**	**7.17**	**0.98**	**<0.001**	**0.05**	**0.51**	**0.53**	**0.026**
Distal BM 176-14	0.33	7.94	0.97	<0.001	0.03	0.51	0.70	0.005
Distal BM 172-14	0.30	5.42	0.97	<0.001	0.02	0.40	0.64	0.009
Distal BM 171-14 Left	0.41	12.66	0.97	<0.001	0.10	0.73	0.68	0.006
Distal BM 171-14 Right	0.35	10.12	0.98	<0.001	0.06	0.62	0.63	0.010
Median of all distal	**0.34**	**9.03**	**0.98**	**<0.001**	**0.04**	**0.67**	**0.67**	**0.007**
Median all proximal and distal	**0.33**	**7.87**	**0.98**	**<0.001**	**0.04**	**0.54**	**0.51**	**0.031**

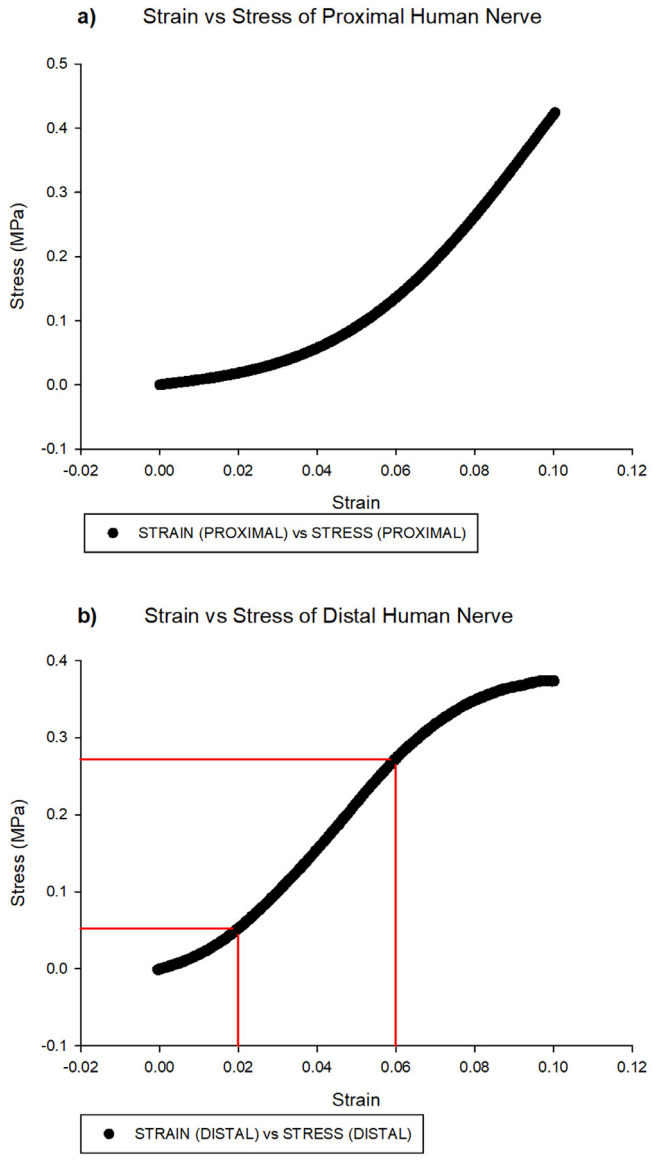

Fig. 3. Stress versus strain of proximal (a) and distal (b) sections of the human ulnar nerve. Stress is measured in MPa while strain is dimensionless. Red lines show 2% and 6% (0.02 and 0.06) strain which corresponds to 0.05 and 0.27 MPa stress. (For interpretation of the references to colour in this figure legend, the reader is referred to the web version of this article.)

Table 3
Estimated strain (%) calculated from the complex (dynamic) modulus (E*). The estimated strain is calculated at the maximum (0.27 MPa) and minimum (0.05 MPa) induced stress (median ± standard deviation).

Frequency (Hz)	E* (MPa)	Strain at 0.05 MPa (%)	Strain at 0.27 MPa (%)
0.5	7.73 ± 2.39	0.65 ± 0.18	3.49 ± 0.99
1	7.89 ± 2.46	0.63 ± 0.18	3.42 ± 0.97
1.5	8.02 ± 2.48	0.62 ± 0.18	3.37 ± 0.96
2	8.09 ± 2.50	0.62 ± 0.18	3.34 ± 0.95
5	8.30 ± 2.53	0.60 ± 0.17	3.25 ± 0.92
10	8.54 ± 2.54	0.59 ± 0.16	3.16 ± 0.85
15	8.78 ± 2.58	0.57 ± 0.15	3.08 ± 0.81
20	8.96 ± 2.48	0.56 ± 0.14	3.01 ± 0.77
24	8.97 ± 2.70	0.56 ± 0.16	3.01 ± 0.85

physiologically relevant frequency range. Except for BM 172-14 E'', all nerves E' and E'' followed an empirical logarithmic frequency-dependent trend. Preliminary data, of the distal nerve, demonstrated that 6% strain was equivalent to 0.27 MPa of stress. This induced stress was selected as the maximum induced stress for dynamic mechanical analysis to ensure no rupture occurred under dynamic loading. The median storage moduli of the proximal nerves ranged between 7.03 and 8.18 MPa for the different frequencies tested. This compared to the range of the distal nerves' median storage modulus which was between 8.85 and 10.19 MPa for the same frequency range. Over the same frequency range, the median loss moduli of the proximal nerves ranged between 0.46 and 0.81 MPa while the range of the distal nerves' median loss modulus was 0.51 and 0.80 MPa. In this preliminary study, no significant differences in viscoelasticity were identified between proximal and distal samples, however, this finding would require confirmation with a larger data set. A larger data set would also allow meaningful comparisons to assess of any gender differences in nerve viscoelasticity.

No consensus exists regarding the critical limit of elongation with various studies ranging from 6% to 100% [16]. From the preliminary test of the distal nerve, the nerve began to rupture at approximately 7–8% strain; this can be seen by a plateau of the induced stress with increased strain. This maximum stress (0.27 MPa) at 6% strain was used to ensure no rupturing occurred during DMA while the stress at 2% strain (0.05 MPa) was used to ensure the nerve specimens were always under tension. A comparison was undertaken to investigate whether the strain measured, from the preliminary ramp test, was comparable with the dynamic "estimated" strain measured by using the complex modulus and induced peak and trough stresses (Eq. (1); see Table 3).

The estimated strain at 0.05 MPa ranged from 0.65 ± 0.18% (0.5 Hz) to 0.56 ± 0.16% (24 Hz) while at 0.27 MPa the estimated strain ranged from 3.49 ± 0.99% (0.5 Hz) to 3.01 ± 0.85% (24 Hz). This estimated strain is different to the preliminary strain (2%, for

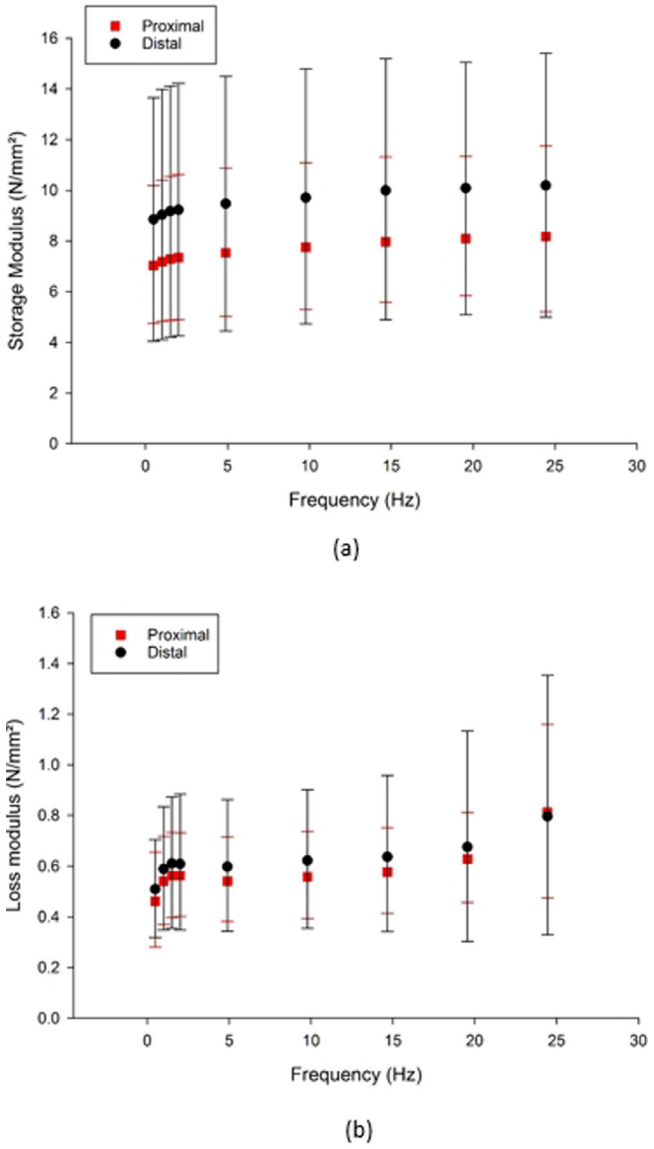

Fig. 4. The proximal and distal ulnar nerve frequency dependent (a) storage modulus (E′) (N/mm^2) and (b) loss modulus (E″) (N/mm^2) (median ± 95% confidence intervals).

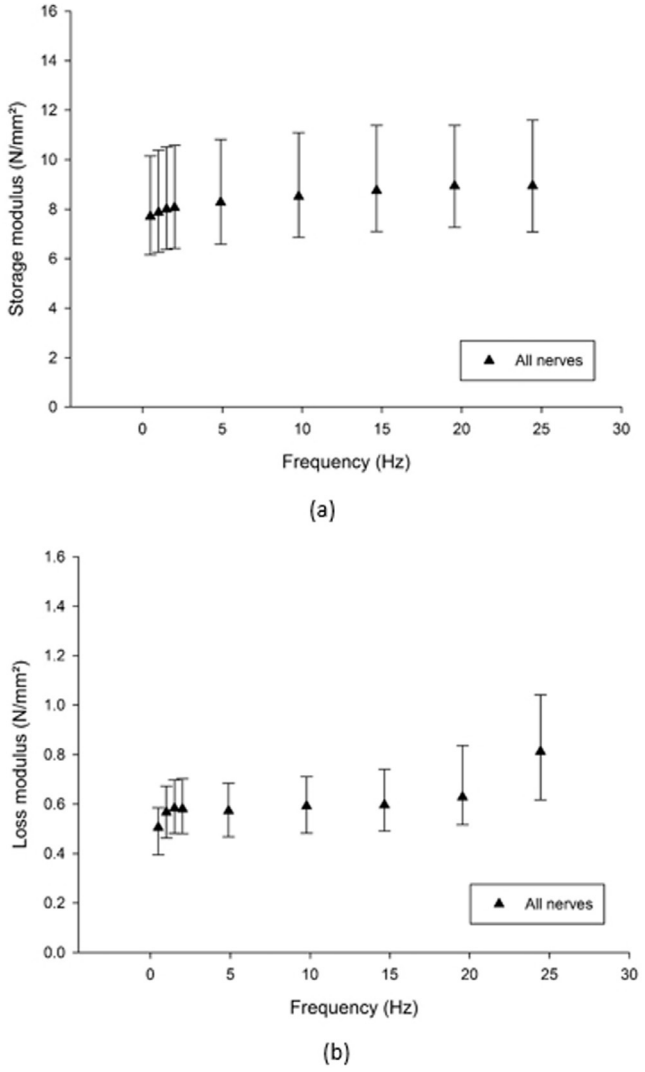

Fig. 5. The ulnar nerve (combined proximal and distal sections) frequency dependent (a) storage modulus (E′) (N/mm^2) and (b) loss modulus (E″) (N/mm^2) (median ± 95% confidence intervals).

0.05 MPa, and 6% for 0.27 MPa). This variation may be due to differences in testing procedure (quasi-static versus dynamic) or may also be due to the linearity assumption of using the complex modulus for the estimated strain [20]. In relation to *in situ* strain of human cadavers, numerous studies have quantified a wide range of strains; 0–17% [15], 0–14% [7], 29% [8], 9–69% [33]. The values estimated in this present study are within these ranges; thus, the viscoelastic measurements provided are within a range which corresponds to existing measures of strain.

To the authors' knowledge, no other studies have investigated the viscoelastic properties (storage modulus and loss modulus) of the ulnar nerve through DMA. Therefore, there is no other literature with which to compare the current results directly. Ma et al. [17] investigated *in vitro* mechanical properties (tensile ramp and stress relaxation tests) of cadaveric nerves as well as measuring *in vivo* stress and deformation intraoperatively. At the same strain, the authors found that the *in vivo* induced stress was over seven times higher than the measured induced stress from the *in vitro* tests [17]. This highlights the different biomechanical properties of a nerve *in situ*, when it is surrounded by connective tissue and still has branches and blood vessels attached, to when it is removed from the body. Further, at 10% strain, Ma et al. [17] calculated that the *in vitro* induced stress, of the ulnar nerve, was approximately 0.18–0.19 MPa while the present study calculated an induced stress of 0.37 MPa (distal) and 0.43 MPa (proximal); approximately 2.0–2.4 times greater. This difference may be due to multiple factors which includes the variability of human tissues, the inconsistency across the testing methodologies and storage/preservation techniques (fresh-frozen [17] versus embalmed (present study).

A potential limitation of the present study is the use of embalmed nerves instead of fresh nerves. Embalmed cadavers were the only type available to use at the time of testing. It is unethical and, therefore, impossible to obtain live human nerves for *in vitro* mechanical testing. Thus, all intact nerves would have had some form of treatment. However, while there is a difference in absolute values between *in situ* biomechanical properties of unembalmed and embalmed ulnar nerves, a correlation in strain values has been previously demonstrated [34]. Another limitation of this study is that only 4 cadavers were available at the time of testing which likely explains the variability seen in the results of this study. This sample size might preclude generalizability. In this study, all

samples were obtained from only 4 nerves; thus, a large difference in means would be necessary, and minimal standard deviation, to detect a difference with significance ($p < 0.05$) when comparing proximal and distal samples. However, our results are consistent with literature where appropriate, and furthermore, clear and consistent trends were obtained.

In this current study, frequency-dependent viscoelasticity has been assessed over a range of 0.5–24 Hz. While much of this range of frequencies may not appear physiological, characterisation of natural tissues should consider not only physiological rates of loading, but also loading associated with exercise, other daily activities, pathophysiology and/or trauma [23,24,35]. However, loading rates and equivalent frequencies associated with loading of the upper-limb/elbow, and of potential relevance to the ulnar nerve are less well understood than, say, for natural tissues such as for heart valves [35–37] or lower limbs [23,38,39]. However, there are upper-limb studies which suggest that frequencies of 20 repeats/min (0.33 Hz) are associated with discomfort levels within a physiological loading range [40], providing a lower range for an experimental loading frequency. Whereas, hand-transmitted vibration for steering wheels have been calculated as having a weighting factor (from an ergonomic perspective) which is greatest between 6 and 25 Hz [41]; peaking at 12.5 Hz. The range of loading frequencies identified from the above studies (0.33 – 25 Hz) is consistent with the range assessed in our study (0.5–24 Hz). However, it is recognised there may be conditions which might expose the nerve to higher loading frequencies not assessed in our study, e.g. 300 Hz [42]. Furthermore, the frequencies used to guide this current study are estimates, as the strain rate of the ulnar nerve itself associated with loading *in vivo* is not currently known. Thus, it is the trend across a range of frequencies (0.5–24 Hz) which is viewed as important in our current study, indicating a frequency range for future studies.

Repeatable characterisation of samples with DMA requires a dynamic “steady-state” [38] to be reached using preconditioning loading cycles. For some natural soft tissues (e.g. articular cartilage) there is evidence that this can require in excess of 1000 loading cycles [43]. However, a minimal number of preconditioning cycles is recommended to avoid the risk of fatigue. In our current study, 28 preconditioning loading cycles were found to enable repeatable viscoelastic characterisation with DMA. Therefore, while 28 cycles may appear high as compared to quasi-static material's characterisation studies (typically employing less than 10 preconditioning loading cycles), it is low as compared to preconditioning used for DMA of natural soft tissues.

Nerves are non-homogenous in nature and structure varies throughout and between individual nerves [16], so the conclusions from this study should be extrapolated only with caution to other nerves, as the measurements may be specific to the ulnar nerve in the region of the cubital tunnel. However, determining the viscoelastic properties of nerves is crucial for choosing suitable nerve grafts, either in manufacturing synthetic grafts or in checking the suitability of allografts. Knowledge of viscoelastic properties is also important in designing and manufacturing diagnostic, surgical and surgical training devices as well as for making computational models for research [25] and for the multi-physics modelling of nerves. Furthermore, a deeper understanding of the mechanical properties of peripheral nerves allows a greater appreciation of mechanisms of nerve injury and repair. It is hoped that such knowledge and equipment will lead to better patient outcomes.

5. Conclusion

The human ulnar nerves display frequency-dependency viscoelasticity. Both the median storage and loss moduli increased logarithmically as the frequency increased, with the storage modulus consistently greater than the loss modulus. Such characterisation is feasible with potential applications to suitable nerve grafts.

Declarations

Ethics approval and consent to participate

Ethical approval was obtained from the Human Tissue Authority according to the Human Tissue Act (2004) under the University of Birmingham license (number 12236) with the donors consenting to the use of their cadavers for education and research. All tissues were obtained following the Declaration of Helsinki ethical principles.

Consent for publication

All donors consented to the use of their cadavers for education and research. This study reports age and gender of donors only.

Competing interests and/or conflicts of interest

None declared.

Funding

This work was supported by Arthritis Research UK through funding for the testing equipment used during this study [Grant Number: H0671]. No funding bodies were involved in the design of the study, collection, analysis, or interpretation of data, nor in writing of the manuscript.

Acknowledgements

The authors would like to express their gratitude to the donors and their families for their altruistic donation to medical education and research. The authors would also like to thank Linda Molanga, Nikita Maria, Max Roderick, Howard Stringer, Priyesh Chauhan and Peter Gaskell for allowing this experiment to be conducted on the cadavers that they were dissecting. Finally, the authors would like to thank Martin Jones, Vicky Cottrell, Amanda Abbott, Kevan Charlesworth, Jack Garrod, Lee Gauntlett, Pete Thornton and Mark Wager for their assistance during dissection and testing.

Supplementary materials

Supplementary material associated with this article can be found, in the online version, at doi:10.1016/j.medengphy.2018.12.009.

References

[1] Drake RL, Vogl AW, Mitchell AWM. Gray's anatomy for students. 2nd ed. Philadelphia: Churchill Livingstone Elsevie; 2010.
[2] Bozentka DJ. Cubital tunnel syndrome. Clin Biomech 1998;351:90–4. doi:10.1016/j.jhsa.2009.11.004.
[3] Apfelberg DB, Larson SJ. Dynamic anatomy of the ulnar nerve at the elbow. Plast Reconstr Surg 1973;51:76–81.
[4] Gelberman RH, Yamaguchi K, Hollstien SB, Winn SS, Heidenreich FP Jr, Bindra RR. Changes in interstitial pressure and cross-sectional area of the cubital tunnel and of the ulnar nerve with flexion of the elbow. An experimental study in human cadavera. J Bone Jt Surg Am 1998;80:492–501.
[5] James J, Sutton LG, Werner FW, Basu N, Allison MA, Palmer AK. Morphology of the cubital tunnel: an anatomical and biomechanical study with implications for treatment of ulnar nerve compression. J Hand Surg Am 2011;36:1988–95. doi:10.1016/j.jhsa.2011.09.014.
[6] Schuind FA, Goldschmidt D, Bastin C, Burny F. A biomechanical study of the ulnar nerve at the elbow. J Hand Surg (British Eur Vol) 1995;20:623–7. doi:10.1016/S0266-7681(05)80124-X.
[7] Toby EB, Hanesworth D. Ulnar nerve strains at the elbow. J Hand Surg Am 1998;23:992–7. doi:10.1016/S0363-5023(98)80005-1.

[8] Wright TW, Glowczewskie F, Cowin D, Wheeler DL. Ulnar nerve excursion and strain at the elbow and wrist associated with upper extremity motion ulnar nerve excursion and strain at the elbow and wrist associated. J Hand Surg Am 2001;26:655–62. doi:10.1053/jhsu.2001.26140.
[9] Cirpar M, Turker M, Yalcinozan M, Eke M, Sahin F. Effect of partial, distal epicondylectomy on reduction of ulnar nerve strain: A cadaver study. J Hand Surg Am 2013;38:666–71. doi:10.1016/j.jhsa.2012.12.033.
[10] Lundborg G, Rydevik B. Effects of stretching the tibial nerve of the rabbit. A preliminary study of the intraneural circulation and the barrier function of the perineurium. J Bone Jt Surg 1973;55:390–401. doi:10.1002/bjs.5095.
[11] Ogata K, Naito M. Blood flow of peripheral nerve effects of dissection stretching and compression. J Hand Surg Am 1986;11:10–14. doi:10.1016/0266-7681(86)90003-3.
[12] Clark WL, Trumble TE, Swiontkowski MF, Tencer AF. Nerve tension and blood flow in a rat model of immediate and delayed repairs. J Hand Surg Am 1992;17:677–87. doi:10.1016/0363-5023(92)90316-H.
[13] Wall EJ, Massie JB, Kwan MK, Rydevik BL, Myers RR, Garfin SR. Experimental stretch neuropathy. Changes in nerve conduction under tension. J Bone Joint Surg Br 1992;74:126–9.
[14] Aoki M, Takasaki H, Muraki T, Uchiyama E, Murakami G, Yamashita T. Strain on the ulnar nerve at the elbow and wrist during throwing motion. J Bone Joint Surg Am 2005;87:2508–14.
[15] Barberio C, Chaudhry T, Power D, Lawless BM, Espino DM, Wilton JC, et al. The effect of shoulder abduction and medial epicondylectomy on ulnar nerve strain. Under Review (Submitted).
[16] Grewal R, Xu J, Sotereanos DG, Woo SL. Biomechanical properties of peripheral nerves. Hand Clin 1996;12:195–204.
[17] Ma Z, Hu S, Tan JS, Myer C, Njus NM, Xia Z. In vitro and in vivo mechanical properties of human ulnar and median nerves. J Biomed Mater Res - Part A 2013;101 A:2718–25. doi:10.1002/jbm.a.34573.
[18] Lawless BM, Barnes SC, Espino DM, Shepherd DET. Viscoelastic properties of a spinal posterior dynamic stabilisation device. J Mech Behav Biomed Mater 2016;59:519–26. doi:10.1016/j.jmbbm.2016.03.011.
[19] Menard KP. Dynamic mechanical analysis. A practical introduction. 2nd ed. Boca Raton, Florida: CRC press. Taylor & Francis Group; 2008.
[20] Hukins DWL, Leahy JC, Mathias KJ. Biomaterials: defining the mechanical properties of natural tissues and selection of replacement materials. J Mater Chem 1999;9:629–36.
[21] Aspden RM. Aliasing effects in Fourier transforms of monotonically decaying functions and the calculation of viscoelastic moduli by combining transforms over different time periods. J Physics D Appl Phys 1991;24:803–8.
[22] Temple DK, Cederlund AA, Lawless BM, Aspden RM, Espino DM. Viscoelastic properties of human and bovine articular cartilage: a comparison of frequency-dependent trends. BMC Musculoskelet Disord 2016;17:419. doi:10.1186/s12891-016-1279-1.
[23] Fulcher GR, Hukins DWL, Shepherd DET. Viscoelastic properties of bovine articular cartilage attached to subchondral bone at high frequencies. BMC Musculoskelet Disord 2009;10:61. doi:10.1016/j.jmbbm.2011.04.018.
[24] Sadeghi H, Espino DM, Shepherd DE. Variation in viscoelastic properties of bovine articular cartilage below, up to and above healthy gait-relevant loading frequencies. Proc Inst Mech Eng Part H J Eng Med 2015;229:115–23. doi:10.1177/0954411915570372.
[25] Barnes SC, Lawless BM, Shepherd DET, Espino DM, Bicknell GR, Bryan RT. Viscoelastic properties of human bladder tumours. J Mech Behav Biomed Mater 2016;61:250–7. doi:10.1016/j.jmbbm.2016.03.012.
[26] Lawless BM, Sadeghi H, Temple DK, Dhaliwal H, Espino DM, Hukins DWL. Viscoelasticity of articular cartilage: analysing the effect of induced stress and the restraint of bone in a dynamic environment. J Mech Behav Biomed Mater 2017;75:293–301. doi:10.1016/j.jmbbm.2017.07.040.
[27] Barnes SC, Shepherd DET, Espino DM, Bryan RT. Frequency dependent viscoelastic properties of porcine bladder. J Mech Behav Biomed Mater 2015;42:168–76. doi:10.1016/j.jmbbm.2014.11.017.
[28] Burton HE, Freij JM, Espino DM. Dynamic viscoelasticity and surface properties of porcine left anterior descending coronary arteries. Cardiovasc Eng Technol 2017;8:41–56. doi:10.1007/s13239-016-0288-4.
[29] Lawless BM, Espino DM, Shepherd DET. In vitro oxidative degradation of a spinal posterior dynamic stabilisation device. J Biomed Mater Res Part B Appl Biomater 2018;106B:1237–44. doi:10.1002/jbm.b.33913.
[30] Kwan MK, Wall EJ, Massie J, Garfin SR. Strain, stress and stretch of peripheral nerve. Rabbit experiments in vitro and in vivo. Acta Orthop Scand 1992;63:267–72. doi:10.3109/17453679209154780.
[31] Topp KS, Boyd BS. Structure and biomechanics of peripheral nerves: nerve responses to physical stresses and implications for physical therapist practice. Phys Ther 2006;86:92–109. doi:10.1177/34.12.3097120.
[32] Bueno FR, Shah SB. Implications of tensile loading for the tissue engineering of nerves. Tissue Eng Part B Rev 2008;14:219–33. doi:10.1089/ten.teb.2008.0020.
[33] Ochi K, Horiuchi Y, Nakamura T, Sato K, Arino H, Koyanagi T. Ulnar nerve strain at the elbow in patients with cubital tunnel syndrome: effect of simple decompression. J Hand Surg (Eur Vol) 2012;38:474–80. doi:10.1177/1753193412465234.
[34] Kleinrensink GJ, Stoeckart R, Vleeming A, Snijders CJ, Mulder PGH, van Wingerden JP. Peripheral nerve tension due to joint motion. A comparison between embalmed and unembalmed human bodies. Clin Biomech 1995;10:235–9. doi:10.1016/0268-0033(95)99800-H.
[35] Wilcox AG, Buchan KG, Espino DM. Frequency and diameter dependent viscoelastic properties of mitral valve chordae tendineae. J Mech Behav Biomed Mater 2014;30:186–95. doi:10.1016/j.jmbbm.2013.11.013.
[36] Baxter J, Buchan KG, Espino DM. Viscoelastic properties of mitral valve leaflets: an analysis of regional variation and frequency-dependency. Proc Inst Mech Eng Part H J Eng Med 2017;231:938–44. doi:10.1177/0954411917719741.
[37] Constable M, Burton HE, Lawless BM, Gramigna V, Buchan KG, Espino DM. Effect of glutaraldehyde based cross-linking on the viscoelasticity of mitral valve basal chordae tendineae. Biomed Eng Online 2018;17:93. doi:10.1186/s12938-018-0524-2.
[38] Espino DM, Shepherd DE, Hukins DW. Viscoelastic properties of bovine knee joint articular cartilage: dependency on thickness and loading frequency. BMC Musculoskelet Disord 2014;15:205. doi:10.1186/1471-2474-15-205.
[39] Sadeghi H, Shepherd DET, Espino DM. Effect of the variation of loading frequency on surface failure of bovine articular cartilage. Osteoarthritis Cartilage 2015;23:2252–8. doi:10.1016/j.joca.2015.06.002.
[40] Mukhopadhyay P, O'Sullivan L, Gallwey TJ. Estimating upper limb discomfort level due to intermittent isometric pronation torque with various combinations of elbow angles, forearm rotation angles, force and frequency with upper arm at 90° abduction. Int J Indust Ergonom 2007;37:313–25. doi:10.1016/j.ergon.2006.11.007.
[41] Goglia V, Gospodaric Z, Kosutic S, filipovic D. Hand-transmitted vibration from the steering wheel to drivers of a small four-wheel drive tractor. App Ergonom 2003;34:45–9. doi:10.1016/S0003-6870(02)00076-5.
[42] Giacomin J, Shayaa MS, Dormegnie E, Richard L. Frequency weighting for the evaluation of steering wheel rotational vibration. Int J Indust Ergonom 2004;33(6):527–41. doi:10.1016/j.ergon.2003.12.005.
[43] Pearson B, Espino DM. Effect of hydration on the frequency-dependent viscoelastic properties of articular cartilage. Proc Inst Mech Eng Part H J Eng Med 2013;227:1246–52. doi:10.1177/0954411913501294.